ERK1/2 Activation in Preexisting Oligodendrocytes of Adult Mice Drives New Myelin Synthesis and Enhanced CNS Function

by

Marisa Adhikusuma Jeffries

B.S., Biology, University of Virginia, 2014

Submitted to the Graduate Faculty of

School of Medicine; Center for Neuroscience at University of Pittsburgh in partial fulfillment

of the requirements for the degree of

M.S. in Neuroscience

University of Pittsburgh

2016

UNIVERSITY OF PITTSBURGH

School of Medicine

This thesis was presented

by

Marisa Adhikusuma Jeffries

It was defended on

December 22, 2016

and approved by

Laura Lillien, Associate Professor, Department of Neurobiology

Quasar Padiath, Assistant Professor, Department of Human Genetics

Thesis Director: Sharyl Fyffe-Maricich, formerly Assistant Professor, Department of Pediatrics

ERK1/2 Activation in Preexisting Oligodendrocytes of Adult Mice Drives New Myelin Synthesis and Enhanced CNS Function

Marisa Adhikusuma Jeffries, M.S.

University of Pittsburgh, 2017

Growing evidence shows that mechanisms controlling CNS plasticity extend beyond the synapse and that alterations in myelin can modify conduction velocity, leading to changes in neural circuitry. Although it is widely accepted that newly generated oligodendrocytes (OLs) produce myelin in the adult CNS, the contribution of preexisting OLs to functional myelin remodeling is not known. Here, we show that sustained activation of extracellular signal-regulated kinases 1 and 2 (ERK1/2) in preexisting OLs of adult mice is sufficient to drive increased myelin thickness, faster conduction speeds, and enhanced hippocampal-dependent emotional learning. Although preexisting OLs do not normally contribute to remyelination, we show that sustained activation of ERK1/2 renders them able to do so. These data suggest that strategies designed to push mature OLs to reinitiate myelination may be beneficial both for enhancing remyelination in demyelinating diseases and for increasing neural plasticity in the adult CNS.

TABLE OF CONTENTS

LIST OF FIGURES

PREFACE

Myelin is a crucial regulator of CNS plasticity, function, and repair. Although it is generally accepted that new myelin production in the adult CNS is initiated by newly generated oligodendrocytes (OLs), great interest remains in additionally driving mature preexisting OLs to make myelin. The ability to induce myelination by the larger population of preexisting OLs carries the potential for enhanced remyelination in demyelinating diseases and increased neural plasticity in the adult CNS. Here, we show that sustained activation of the extracellular signal-regulated kinases 1 and 2 (ERK1/2) signaling pathway is sufficient to drive mature OLs in the adult mouse CNS to reinitiate myelination, leading to new myelin wraps and functional changes.

We thank Mara Sullivan and the Center for Biologic Imaging at University of Pittsburgh for assistance in obtaining transmission EM sections and images; Laura Miller, Edda Thiels, and the Rodent Behavioral Analysis Core at the University of Pittsburgh for assistance in performing behavior tests and analyzing data; Luther Loose and Shil Patel for technical assistance in experiments; and Stephen Maricich, Jenna Gaesser, and Lilly Laemmle for helpful discussion and comments on this manuscript. I personally thank my mentor, Dr. Sharyl Fyffe-Maricich, for her irreplaceable guidance and support in the completion of this master's thesis.

1.0 INTRODUCTION

Myelin, the specialized membrane that wraps concentrically around axons, greatly speeds neurotransmission by enabling efficient action potential propagation. In the CNS, myelin is produced by oligodendrocytes (OLs), the majority of which develop from a proliferative population of oligodendrocyte progenitor cells (OPCs) early in postnatal development. However, a small population of OPCs (5% of all CNS cells; Dawson et al., 2003) persists throughout adulthood and provides a continual source of new OLs that generate myelin (Young et al., 2013). Myelination is dynamically regulated by neuronal activity (Demerens et al., 1996; Stevens et al., 1998; Stevens et al., 2002; Dimou et al., 2008; Rivers et al., 2008; Psachoulia et al., 2009; Wake et al., 2011; McKenzie et al., 2014) and changes in myelin thickness, length, and axonal coverage patterns are thought to contribute to fine tuning of neuronal networks by altering the synchronicity of impulse conduction between distant cortical regions (Waxman, 1980, 1997). In fact, new myelin produced by recently differentiated OPCs is required for motor skill learning in mice (McKenzie et al., 2014). New myelin is also generated throughout life in humans, but the low rate of OL turnover suggests that myelin remodeling is performed primarily by mature OLs (Yeung et al., 2014). MRI studies show that white matter changes occur in association with cognitive development (Fields, 2008), during language learning (Schlegel et al., 2012), and after a few weeks of practicing a new skill (Bengtsson et al., 2005; Scholz et al., 2009). Together, these studies point to a role for myelin plasticity in learning and memory. The extent to which

functional myelin remodeling in the adult CNS is mediated by newly generated OLs compared with new membrane produced by preexisting OLs remains unclear. A series of recent, elegant studies show that remyelination, the regenerative response to demyelination in the CNS, is also mediated by newly generated OLs (Kang et al., 2010; Tripathi et al., 2010; Zawadzka et al., 2010), with no contribution from preexisting OLs (Gensert and Goldman, 1997; Keirstead and Blakemore, 1997; Fancy et al., 2004; Crawford et al., 2016). Because differentiating OPCs often become arrested at premyelinating stages during the progressive phase of demyelinating diseases such as multiple sclerosis (Chang et al., 2002; Sim et al., 2002) and the pool of OPCs present in the adult brain is relatively small, it is important to investigate whether the large pool of existing OLs retains any potential for myelin production in the adult CNS. We and others have shown that the extracellular signal-regulated kinases 1 and 2 (ERK1/2) are critical for proper myelination during development (Ishii et al., 2012; Fyffe-Maricich et al., 2013; Ishii et al., 2013). In the adult, sustained activation of ERK1/2 in OPCs improves remyelination (Fyffe-Maricich et al., 2013) and ERK1/2 signaling is crucial for the maintenance of myelin (Ishii et al., 2014). In this study, we investigated the effects of sustained ERK1/2 activation in preexisting adult OLs by using tamoxifen-inducible transgenic mice that express a constitutively active variant of the ERK1/2 upstream kinase, MEK1, specifically in proteolipid protein (PLP)-expressing OLs (Plp-CreERT;Mek1DD/). We found that increased levels of activated ERK1/2 in mature OLs resulted in increased myelin thickness, faster conduction speeds, and enhanced contextual fear conditioning. Sustained activation of ERK1/2 also enabled preexisting OLs to contribute to remyelination. Although it is accepted that newly differentiated OLs contribute to myelin plasticity and repair, our studies provide what is, to our knowledge, the first direct

evidence that myelin derived from preexisting OLs can also lead to functional changes in both the injured and uninjured adult CNS.

1.1 THE ROLE OF ENHANCED ERK1/2 ACTIVATION IN MATURE OLIGODENDROCYTES OF THE ADULT CNS

1.1.1 Sustained activation of ERK1/2 in OLs of adult mice drives myelin sheath expansion through the addition of new myelin to existing sheaths

WT;Mek1DD/+ (WT) and *Plp-Cre^{ERT};Mek1DD/+* (MUT) littermate mice were injected with tamoxifen at adulthood (P60) to induce recombination and the subsequent expression of MEK1DD. Mice were harvested either 21 days (dpi) or 2 months post-injection (mpi). Immunostaining using antibodies against CC1 (a marker of mature OLs) and GFP (a reporter of MEK1DD expression) indicated that ~60% of OLs expressed MEK1DD in both spinal cord white matter and the corpus callosum, consistent with recombination rates reported in previous studies using *Plp-Cre^{ERT}* mice (Guo et al., 2010). To confirm that the expression of MEK1DD drove enhanced phosphorylation of ERK1/2 (pERK1/2) in mature OLs, tissue sections from the corpus callosum and spinal cord at 2 mpi were double-immunostained with antibodies against CC1 and pERK1/2. The percentage of mature OLs that co-labeled for pERK1/2 in *Plp-Cre^{ERT};Mek1DD/+* mice was significantly increased compared to littermate controls in both the spinal cord (WT = 15.5 ± 2.9%, MUT = 55.0 ± 3.2%, p = 0.0001) and corpus callosum (WT = 12.4 ± 2.8%, MUT = 30.9 ± 1.9%, p = 0.008) (Fig. 1A-B). Interestingly, the percentage of

pERK1/2+ OLs was significantly lower in the corpus callosum than in the spinal cord of mutant mice ($p = 0.0007$), despite the fact that recombination rates were similar in both tissues. Additionally, analysis of pERK immunostaining intensity in individual CC1+ cells confirmed that mutant mice displayed a significant 176.59% increase in pERK levels in the spinal cord and 34.27% increase in the corpus callosum. Finally, numbers of mature OLs did not differ between *Plp-Cre^{ERT};Mek1DD/+* and control littermates in either the dorsal column of the spinal cord (WT = 83.1 ± 7.1, MUT = 89.2 ± 4.2, $p = 0.51$) or corpus callosum (WT = 78.4 ± 4.1, MUT = 78 ± 6.3, $p = 0.96$), suggesting that increased levels of pERK1/2 do not affect baseline OL survival (Fig. 1C).

To determine whether increased pERK1/2 expression was sufficient to cause hypermyelination and white matter tract expansion, matched sections from spinal cord and brain were immunostained for proteolipid protein (PLP), a major myelin protein. *Plp-Cre^{ERT};Mek1DD/+* mice displayed a dramatic expansion of the thoracic spinal cord white matter accompanied by subtle expansion of the medial and lateral aspects of the corpus callosum (Fig. 1D). Myelin thickness was assessed using electron microscopy (EM) followed by g-ratio calculation (axon diameter/total outer diameter of myelinated fiber). *Plp-Cre^{ERT};Mek1DD/+* mice demonstrated significantly lower g-ratios (thicker myelin) at 21 dpi in both spinal cord (WT = 0.754 ± 0.003, MUT = 0.719 ± 0.004, $p = 9.69 \times 10^{-11}$) and corpus callosum (WT = 0.768 ± 0.003, MUT = 0.746 ± 0.003, $p = 4.18 \times 10^{-8}$) (Fig. 1E, G-J). Additionally, myelin thickness increased slowly over time in the mutant spinal cord as demonstrated by a decrease in the g-ratio with increasing age (21 dpi MUT = 0.719 ± 0.004, 2 mpi MUT = 0.701 ± 0.004, $p = 0.002$) (Fig. 1G, I). Average g-ratios in the corpus callosum showed a similar trend of decreasing over time (21 dpi MUT = 0.746 ± 0.003, 2 mpi MUT = 0.738 ± 0.004, $p=0.06$) (Fig. 1H, J). High power

magnification revealed similar myelin ultrastructure between mutant mice and control littermates, demonstrating that the increased myelin thickness was due to the addition of new myelin wraps (Fig. 1F). Importantly, similar numbers of mature OLs in *Plp-Cre^{ERT};Mek1DD/+* and control littermates suggests that the increased myelin thickness in mutants resulted from enhanced myelin production by individual OLs (Fig. 1C).

The adult corpus callosum contains >70% unmyelinated axons (Sturrock, 1980), making it difficult to determine whether sustained ERK1/2 activation drove myelination of normally unmyelinated axons or addition of myelin to existing sheaths. To distinguish between these possibilities, we examined adult mouse optic nerve, which consists almost entirely of myelinated axons (Bartsch et al., 1997; Dangata and Kaufman, 1997; Honjin et al., 1977). If excess pERK1/2 solely enabled OLs to myelinate normally unmyelinated axons, then we would not expect to see hypermyelination in the optic nerve. However, EM analysis of optic nerve at 2 mpi revealed significantly decreased g-ratios in *Plp-Cre^{ERT};Mek1DD/+* mice compared to control littermates (WT = 0.750 ± 0.003, MUT = 0.714 ± 0.003, $p = 8.73 \times 10^{-16}$), suggesting that increased pERK1/2 drives addition of new myelin to existing sheaths (Fig. 1K-M). Furthermore, analysis of electron micrographs from 2 mpi spinal cord and corpus callosum revealed no significant differences in the relative numbers of unmyelinated axons between *Plp-Cre^{ERT};Mek1DD/+* and *WT;Mek1DD/+* mice (Fig. 1M). These data indicate that sustained ERK1/2 activation induces addition of new myelin to existing sheaths rather than *de novo* myelination of naked axons.

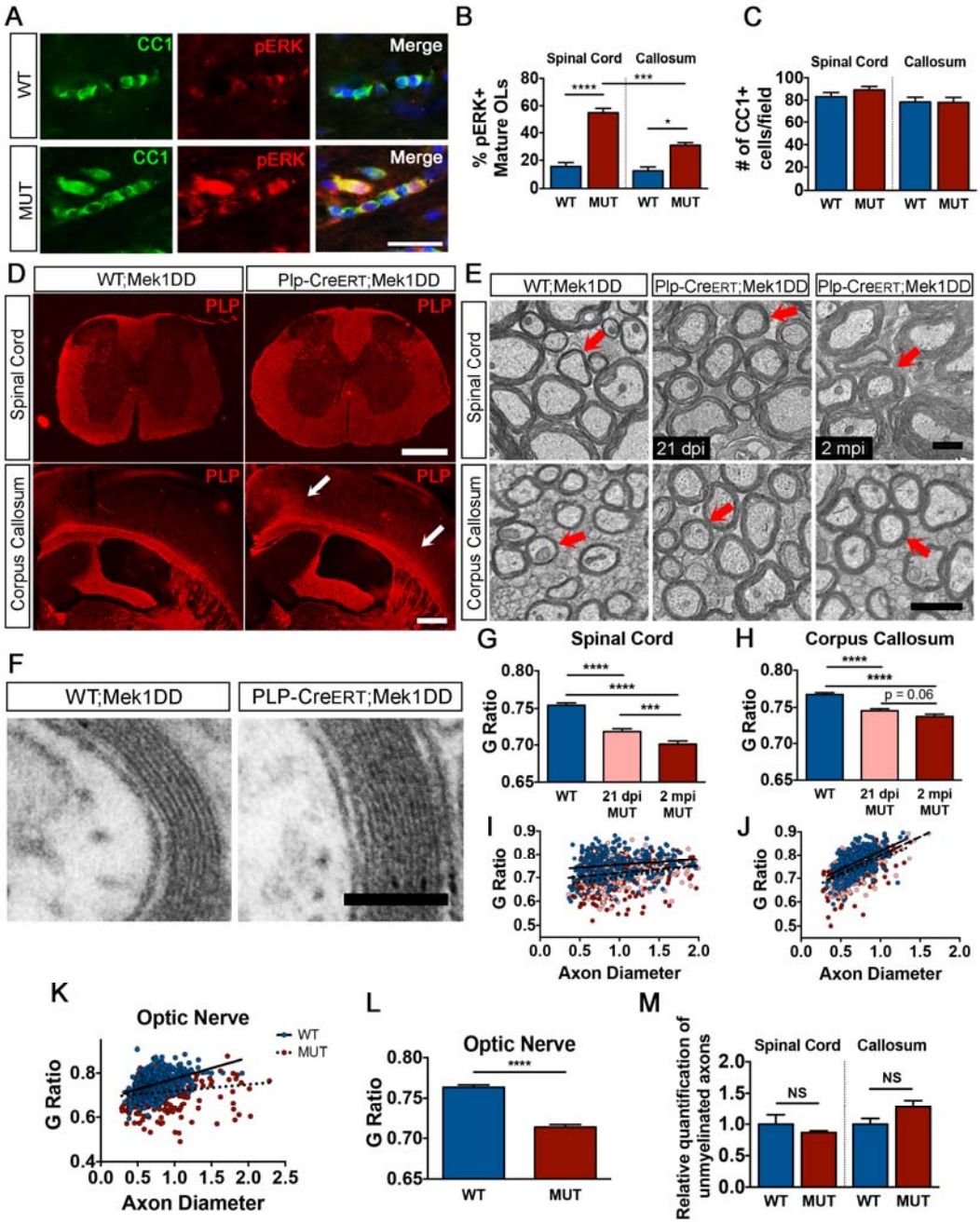

Figure 1. ***Plp-Cre^{ERT}; Mek1DD/+*** **mice demonstrate increased myelin thickness as a result of the addition of new myelin wraps to existing myelin sheaths.**

A, Matched corpus callosum (CC) sections from adult *WT;Mek1DD/+* (WT) and *Plp-Cre^{ERT};Mek1DD/+* (MUT) mice at 2 months post-tamoxifen injection (mpi) stained with CC1 (green) and pERK (red). Scale bar, 25 µm. **B,** Quantification confirms a significant increase in

the percentage of CC1+ cells that co-labeled with pERK in MUT mice in both spinal cord (SC) and CC. **C,** Quantification of the total number of CC1+ mature OLs in the dorsal column of the SC and the CC at 2 mpi demonstrates no significant difference between WT and MUT mice. **D,** Matched SC and CC sections immunolabeled with anti-PLP reveal enlargement of white matter structures in MUT mice. Arrows point to expanded areas of the CC. Scale bars, 500 µm. **E,** Electron micrographs of SC and CC show increased myelin thickness in MUT mice compared to control littermates at 21 days post injection (dpi) and at 2 mpi. Arrows indicate example axons of similar diameter. Scale bar for SC, 2 µm; CC, 1 µm. **F,** High magnification electron micrographs reveal that the additional myelin wraps seen in MUT mice appear ultrastructurally normal. Scale bar, 100 nm. **G-H,** Analysis of SC electron micrographs by g-ratio calculation shows significantly decreased g-ratios (thicker myelin) in both 21 dpi MUT (pink) and 2 mpi MUT (red) mice compared to WT (blue) controls, with a significant decrease from 21 dpi to 2 mpi. **I-J,** G-ratio calculation from CC electron micrographs indicates significantly decreased g-ratios in both 21 dpi MUT (pink) and 2 mpi MUT (red) mice compared to WT (blue) controls. **K,** Analysis of optic nerve (ON) EM micrographs shows significantly decreased g-ratios in 2 mpi MUT (red) mice compared to WT (blue) controls. **L,** Average ON g-ratios show overall significantly decreased g-ratios observed in MUT (red) mice versus WT (blue) controls. **M,** Examining the number of unmyelinated axons in SC and CC electron micrographs shows no difference between WT (blue) and 2 mpi MUT (red) mice. ****$p<0.0001$, ***$p<0.001$, *$p<0.05$. Data are mean ± SEM. NS = not significant. At least 3 mice per genotype were used for all analyses; at least 100 axons per mouse were analyzed for g-ratio calculations.

1.1.2 Global hypermyelination in *Plp-Cre^{ERT};Mek1DD/+* mice is largely mediated by preexisting mature OLs

Although the *Plp* promoter is active primarily in mature OLs, adult *Plp-Cre^{ERT}* mice also express Cre recombinase in a small percentage (5-20%) of OPCs (Guo et al., 2010). These data raise the possibility that the hypermyelination observed in the *Plp-Cre^{ERT};Mek1DD/+* mice may be mediated by excess myelin generated by a small population of recently differentiated MEK1DD+ adult OPCs rather than by pre-existing OLs. To address this question, we used an inducible *Pdgfrα-Cre^{ERT}* (Kang et al., 2010) to express MEK1DD specifically in adult OPCs. Tamoxifen was administered to adult (P60) *WT;Mek1DD/+* (WT) and *Pdgfrα-Cre^{ERT};Mek1DD/+* (MUT2) mice to induce recombination. Double-immunostaining for GFP and the OPC marker NG2 in MUT2 mouse corpus callosum confirmed that a large number (~55%) of OPCs had recombined following injection with tamoxifen (Fig. 2A). Over the course of 2 months, these recombined OPCs differentiated into mature CC1+ OLs that expressed high levels of pERK1/2 (Fig. 2B) and made up ~20% of the total mature OL population, in line with previous work examining adult OPC differentiation in WT mice (Young et al., 2013). These results suggest that the increased pERK did not result in accelerated differentiation, which is also in line with previously published in vivo studies (Fyffe-Maricich et al., 2013; Ishii et al., 2013). Immunostaining of matched spinal cord sections at 2 mpi using antibodies against myelin basic protein (MBP) revealed that the overall size of the white matter appeared similar across genotypes, suggesting that upregulation of pERK1/2 in adult OPCs is not sufficient to cause white matter expansion within this time frame (Fig. 2C). Additionally, EM analysis of the corpus callosum at 2 mpi demonstrated comparable g-ratios between *WT;Mek1DD/+* and *Pdgfrα-Cre^{ERT};Mek1DD/+* mice (WT = 0.770 ± 0.002,, MUT2 = 0.771 ± 0.003, p = 0.72) (Fig. 2D-E). Therefore, we conclude

that new myelin generated by pre-existing, mature OLs in the *Plp-Cre^{ERT};Mek1DD/+* mice must contribute significantly to the hypermyelination phenotype.

Although overall myelin thickness was not altered in the *Pdgfrα-Cre^{ERT};Mek1DD/+* mice, we hypothesized that increased levels of pERK1/2 were sufficient to drive increased thickness of new myelin sheaths that was undetectable globally. To test this hypothesis, *Pdgfrα-Cre^{ERT};Mek1DD/+* mice were crossed to reporter mice that express a membrane bound GFP following Cre-mediated recombination (*Tau-lox-mGfp-Ires-Nls-LacZ-pA)* (Hippenmeyer et al., 2005) so that myelin generated by newborn OLs is labeled green. Myelin produced by newborn OLs with sustained activation of ERK1/2 (mGFP signal localized to the inner tongue, but was excluded from compact myelin as seen in (Young et al., 2013)) appeared thick, visualized by an expansion of the MBP signal when compared to adjacent axons of similar caliber that were mGFP negative (Fig. 2F). More than 70 mGFP+ myelinated axons were visually analyzed and compared to non-mGFP+ myelinated axons. The majority of mGFP+ myelinated axons appeared visibly thicker (79.92 ± 1.37%), and those that did not were likely the result of de novo myelination that had just begun. These data suggest that increased levels of pERK1/2 are sufficient to drive excess myelin production by newly generated OLs in the adult CNS in line with previously published studies using *Cnp-Cre; Mek1DD/+* mice (Fyffe-Maricich et al., 2013; Ishii et al., 2013), however, due to the fact that the amount of new myelin produced over the 2 month period is such a small percentage of the total amount of CNS myelin, the hypermyelination remains undetectable on a global level.

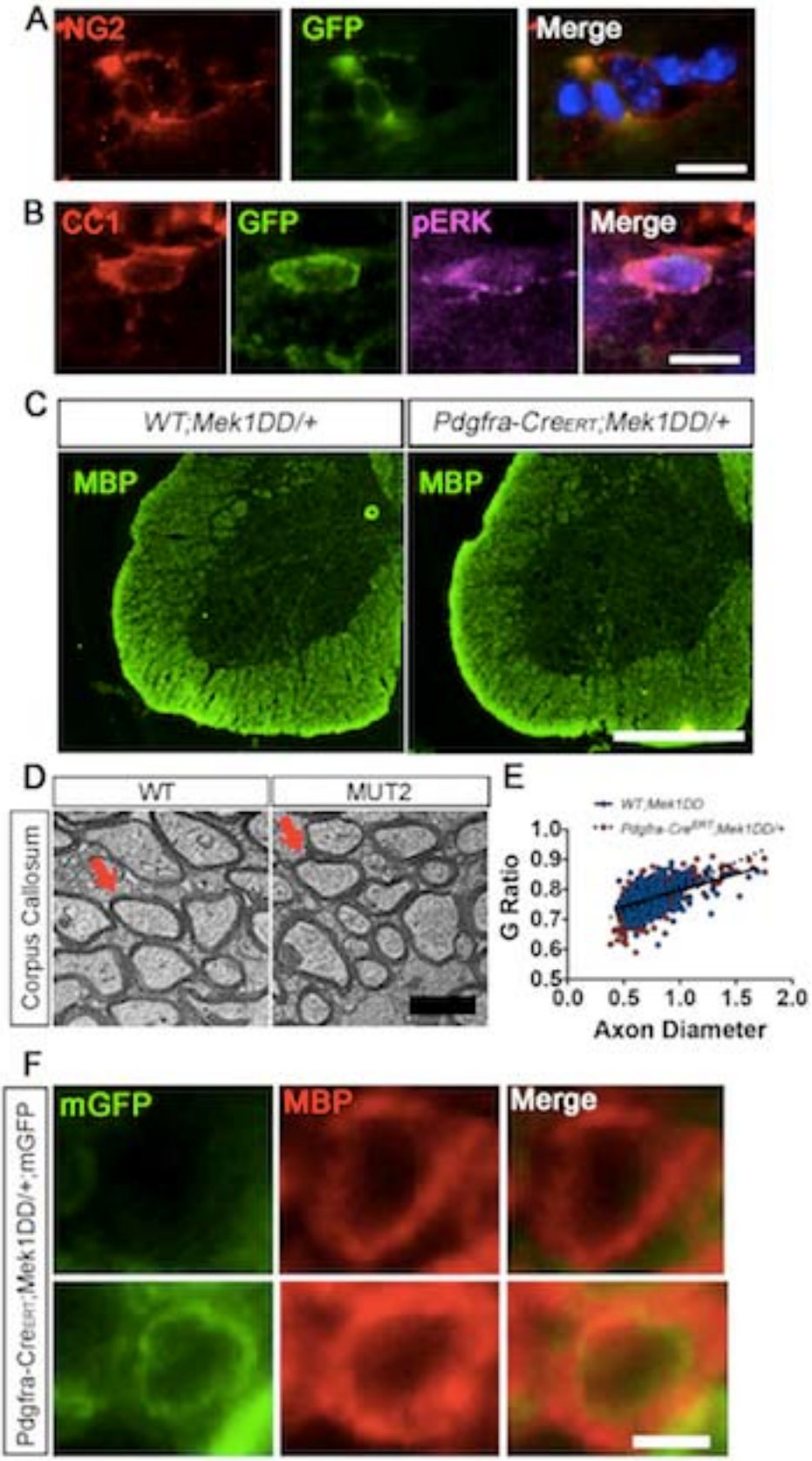
A
NG2
GFP
Merge
B
CC1
GFP
pERK
Merge
C
WT;Mek1DD/+
Pdgfra-CreERT;Mek1DD/+
MBP
MBP
D
WT
MUT2
Corpus Callosum
E
WT;Mek1DD
Pdgfra-CreERT;Mek1DD/+
G Ratio
1.0
0.9
0.8
0.7
0.6
0.5
0.0
0.5
1.0
1.5
2.0
Axon Diameter
F
Pdgfra-CreERT;Mek1DD/+;mGFP
mGFP
MBP
Merge

Figure 2. **Increased pERK1/2 in adult OPCs, but not pre-existing OLs, does not cause global hypermyelination.**

A, Immunostaining of *Pdgfrα-Cre^{ERT};Mek1DD/+* corpus callosum with antibodies against NG2 (red) and GFP (green) confirms that adult OPCs have recombined to activate the expression of MEK1DD and the GFP reporter. DAPI marks cell nuclei in blue. Scale bar, 10 μm. **B**, CC1, GFP, and pERK triple immunostaining of 2 mpi *Pdgfrα-Cre^{ERT};Mek1DD/+* corpus callosum confirms that MEK1DD expressing adult OPCs differentiate into mature oligodendrocytes with elevated pERK1/2. DAPI marks cell nuclei in blue. Scale bar, 10 μm. **C**, MBP immunostaining of matched spinal cord sections from *WT;Mek1DD/+* and *Pdgfra-Cre^{ERT};Mek1DD/+* mice at 2 mpi demonstrates that there is no significant expansion of the white matter tracts. Scale bar, 500 μm. **D**, Electron micrographs from the corpus callosum at 2 mpi reveals comparable myelin thickness in *WT;Mek1DD/+* and *Pdgfra-Cre^{ERT};Mek1DD/+* mice. Scale bar, 2 μm. Arrows indicate representative axons. **E**, Scatter plot depicting similar g-ratios from *WT;Mek1DD/+* (blue) and *Pdgfra-Cre^{ERT};Mek1DD/+* (red) mice in relation to axon diameter. **F**, Immunostaining with antibodies against MBP and mGFP reveals thicker myelin produced by a recombined newly-generated OL versus an unrecombined OL. Scale bar, 1 μm. At least 3 mice per genotype were used for all analyses; at least 100 axons per mouse were analyzed for g-ratio calculations.

1.1.3 ERK1/2 signaling in mature OLs drives the production of both myelin proteins and lipids

Previous studies from our lab and others show that ERK1/2 signaling is necessary for transcription of MBP and PLP (Ishii et al., 2014; Ishii et al., 2012) and for translation of MBP after demyelination (Michel et al., 2015). To determine whether sustained ERK1/2 activation in

mature OLs of the adult CNS is sufficient to drive increased transcription and/or translation of major myelin proteins, we quantified protein expression from *Plp-Cre^{ERT};Mek1DD/+* and *WT;Mek1DD/+* cortex and underlying corpus callosum at 2 mpi using western blot analysis. Mutant mice exhibited significant increases in myelin oligodendrocyte glycoprotein (MOG) and PLP expression compared to control littermates (Fig. 3A-B). While overall levels of MBP were not significantly increased ($p = 0.27$), separate examination of heavy (21.5 kDa) and light (18 kDa) MBP isoforms revealed a significant increase specifically in the 18 kDa isoform (27.9 ± 10.7%, $p = 0.04$) (Fig. 3B). In order to determine whether these changes in myelin protein expression were the result of transcriptional changes, we next performed qRT-PCR and found significant increases in *Mog* and *Plp* mRNA expression (Fig. 3C). However, *Mbp* levels were comparable between *Plp-Cre^{ERT};Mek1DD/+* and *WT;Mek1DD/+* controls, suggesting that regulation of MBP occurs at the level of translation in these mice (Fig. 3C).

While myelin is composed of roughly 20% protein, the remaining 80% is made up of lipids, one of which is galactosylceramide (GalC), a glycosphingolipid commonly used to identify OLs. GalC and its sulfated derivative make up nearly 30% of the lipid content of myelin (Norton and Cammer, 1984). To determine whether elevated levels of pERK1/2 in OLs increase myelin lipids, GalC species were quantified in the *Plp-Cre^{ERT};Mek1DD/+* corpus callosum at 2 mpi. Total GalC (defined as the sum of the four most prevalent GalC species in the CNS; d18:1/22:1, d18:1/24:1, d18:1/22:0, and d18:1/24:0) was increased by 68.3 ± 12.5% ($p = 0.007$) in mutants compared to littermate controls. Separate analysis of each of the GalC species also revealed significant increases in d18:1/22:0, d18:1/22:1, and d18:1/24:1 (Fig. 3D).

Deletion of *Erk1/2* from mature OLs of adult mice causes downregulation of myelin regulatory factor (*Myrf*), a master transcriptional regulator of myelin proteins, and ceramide UDP-

galactosyltransferase (*Cgt*), an enzyme critical for GalC synthesis (Ishii et al., 2014). To determine whether sustained ERK1/2 activation upregulated *Myrf* and/or *Cgt* transcription, we performed qRT-PCR using cDNA from cortex and underlying corpus callosum of *WT;Mek1DD/+* and *Plp-Cre^{ERT};Mek1DD/+* mice at 2 mpi. *Myrf* and *Cgt* transcript levels were increased by 36.9 ± 6.5% ($p = 0.04$) and 122.5 ± 33.3% ($p = 0.03$), respectively, in *Plp-Cre^{ERT};Mek1DD/+* mice (Fig. 3E). Since these transcriptional changes were observed at the relatively late time point of 2 mpi, we wondered whether *Myrf* and *Cgt* were likely to be direct targets of ERK1/2 or whether they were simply upregulated as a secondary consequence of actively growing myelin sheaths. To address this question, transcript levels were quantified from corpus callosum using qRT-PCR 4 days after the last dose of tamoxifen (14 dpi). At this relatively early time point, *Myrf* mRNA levels were comparable in *Plp-Cre^{ERT};Mek1DD/+* mice and control littermates, while *Cgt* transcript levels were increased by 47.8 ± 11.9% ($p = 0.04$) (Fig. 3F). These data show that ERK1/2 activation in OLs of adult mice causes early and sustained increases in *Cgt* transcription, leading to increased production of the major myelin lipid GalC. The fact that changes in *Myrf* transcript levels are not detected at the early time point suggests that *Myrf* may not be a primary target of ERK1/2 signaling.

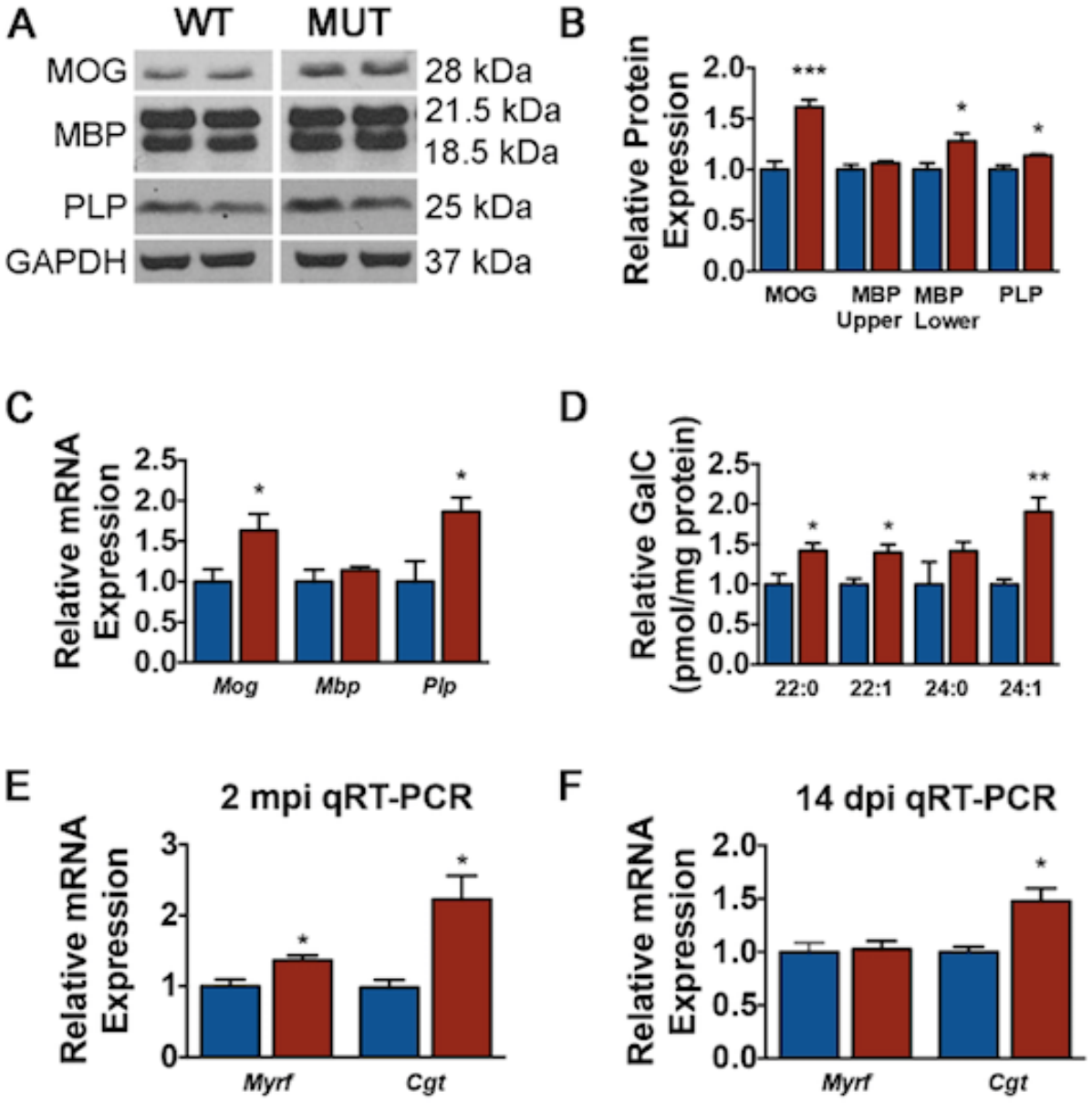

Figure 3. **Enhanced ERK1/2 signaling in mature OLs of adult mice drives the synthesis of excess myelin proteins and lipids.**

A-B, Western blot analysis of corpus callosum and overlying cortex at 2 mpi reveals increased levels of the myelin proteins MOG, PLP, and the 18.5 kDa isoform of MBP in *Plp-Cre^{ERT};Mek1DD/+* (MUT) mice compared to *WT;Mek1DD/+* (WT) littermate controls**. C,**

Quantitative RT-PCR from corpus callosum and overlying cortex at 2 mpi shows significantly increased *Mog* and *Plp* transcripts in MUT (red) mice compared to WT (blue) controls. **D,** Quantification of the major myelin lipid galactosylceramide (GalC) species using mass spectrometry shows a significant increase in the relative concentration of GalC in MUT (red) compared to WT (blue) corpus callosum, each d18:1 species is normalized to itself in WT. **E,** Quantitative RT-PCR results demonstrate a significant upregulation of *Myrf* and *Cgt* at 2 mpi in MUT (red) mice. **F,** Similar quantitative RT-PCR analysis at an earlier time point of 14 dpi indicates a significant increase in *Cgt* but not *Myrf* in MUT (red) corpus callosum compared to littermate (blue) controls. ***p<0.001, **p<0.01, *p<0.05. Data are mean ± SEM. Four to five mice per genotype were used for Western blot analysis; at least 3 mice per genotype were used for qRT-PCR and LC-MS/MS analysis.

1.1.4 *Plp-Cre^{ERT};Mek1DD/+* mice develop expanded paranodal regions but shorter nodes of Ranvier

Nodes of Ranvier along myelinated axons are small regions between individual myelin internodes where the axonal membrane and its clustered Na^+ channels are exposed to the extracellular space. During myelin growth, the innermost tongue of the myelin sheath spirally wraps the axon, resulting in addition of new myelin layers with lateral cytoplasm-containing edges. Each new layer then extends longitudinally, pushing the lateral cytoplasmic loops toward the edges of the myelin sheath until they finally align in a set of closely apposed paranodal loops (Snaidero et al., 2014). Therefore, we set out to determine whether the increased levels of pERK1/2 re-initiated myelin growth in mature OLs by driving the inner tongue forward, creating excess myelin wraps and additional paranodal loops. If this were true, then we would expect to

find expanded paranodal regions in *Plp-Cre^{ERT};Mek1DD/+* mice. Coronal brain sections of *Plp-Cre^{ERT};Mek1DD/+* mice and littermate controls at 2 mpi were immunostained using antibodies against contactin-associated protein (CASPR) and Na^+ channel 1.6 (NaV1.6) in order to visualize and then measure paranodal and nodal lengths, respectively, in the corpus callosum (Fig. 4A). CASPR immunostaining was significantly longer in *Plp-Cre^{ERT};Mek1DD/+* mice compared to littermate controls (WT = 3.68 ± 0.05 µm, MUT = 3.87 ± 0.05 µm, p = 0.04) (Fig. 4C), while NaV1.6 immunostaining was significantly shorter (WT = 1.14 ± 0.01 µm, MUT = 1.02 ± 0.02 µm, p = 0.02) (Fig. 4D). The absolute number of nodes of Ranvier, however, was unchanged (WT = 87.8 ± 3.3, MUT = 83.4 ± 6.5, p = 0.60) (Fig. 4B). These data suggest that the average internode length increases slightly in *Plp-Cre^{ERT};Mek1DD/+* mice due to an expansion of the paranodal region, which is in contrast to the decrease in the length of myelin internodes produced by newly generated OLs in the adult CNS (Young et al., 2013). EM analysis of the paranodal regions in the corpus callosum demonstrated suitable adhesion between the innermost paranodal loops and the axolemma in mutant mice and did not reveal any notable ultrastructural abnormalities (Fig. 4E). These data indicate that sustained ERK1/2 activation in *Plp-Cre^{ERT};Mek1DD/+* mice drives addition of new myelin wraps to existing sheaths, resulting in new paranodal loops that are appropriately anchored to the axon accompanied by concurrent shortening of the nodal region. Together, these changes result in an overall stable density of nodes.

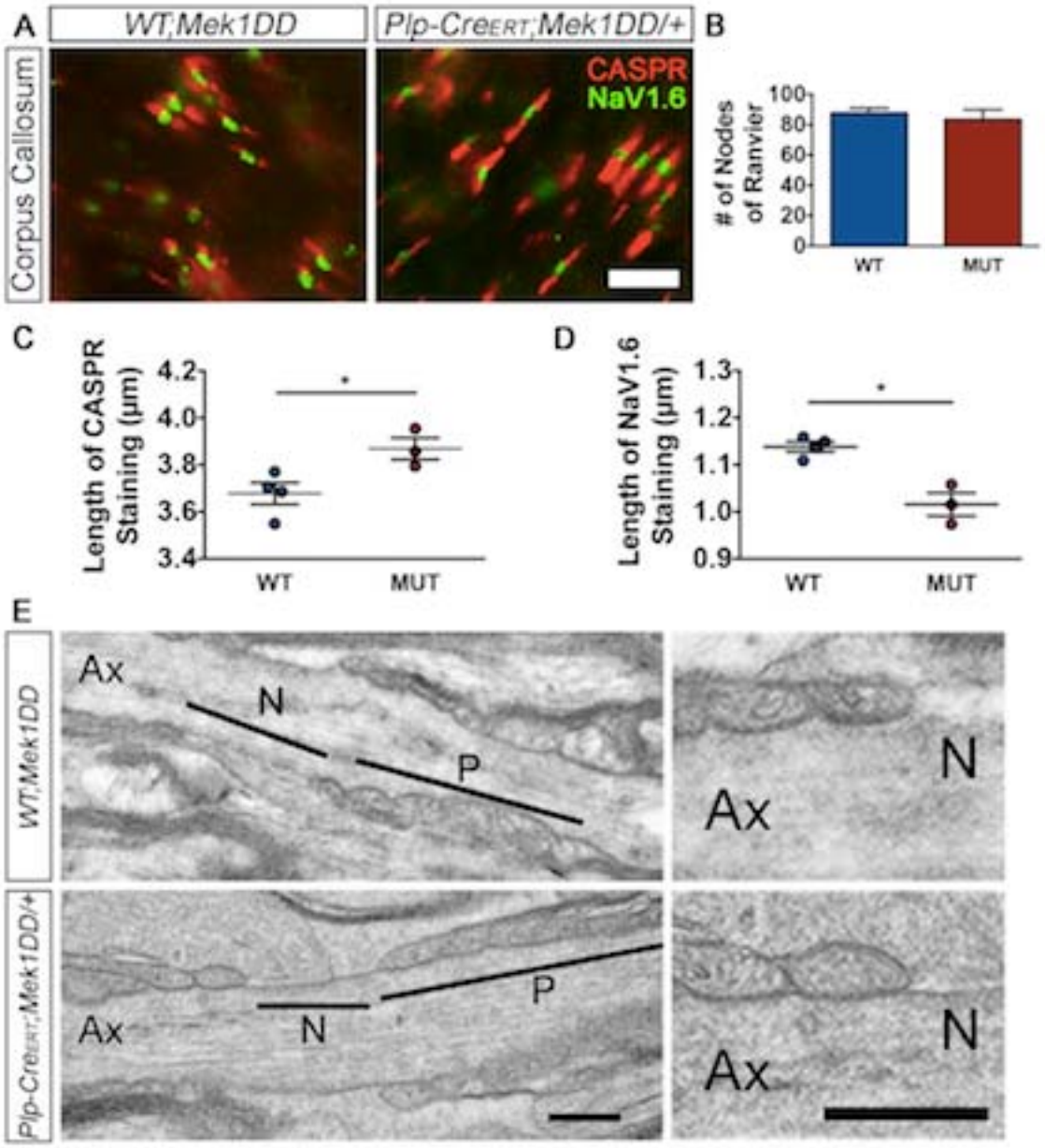

Figure 4. **ERK1/2-mediated hypermyelination results in reciprocal changes to the length of the nodal and paranodal regions.**

A, CASPR (red) and NaV1.6 (green) immunostaining of matched sections of corpus callosum from *WT;Mek1DD/+* (WT) and *Plp-Cre^{ERT};Mek1DD/+* (MUT) littermates at 2 mpi. Scale bar, 5 µm. **B,** Quantification of the number of Nodes of Ranvier demonstrates a comparable overall density of nodes in WT and MUT mice. **C,** Measurement of the length of CASPR staining

indicates an increase in paranode length in MUT mice, while measurement of NaV1.6 staining (**D**) reveals a concurrent decrease in node length in MUT corpus callosum. **E,** High magnification electron micrographs of representative paranodes from corpus callosum demonstrate a comparable ultrastructure of WT and MUT paranodes. Ax = axon, N = node, P = paranode. Scale bars, 400 nm. *p<0.05. Data are mean ± SEM. At least 3 mice per genotype were used for all analyses; at least 100 nodes or paranodes per mouse were measured for length analysis.

1.2 THE FUNCTIONAL CONSEQUENCES OF SUSTAINED ERK1/2 ACTIVATION IN MATURE OLIGODENDROCYTES OF THE ADULT CNS

1.2.1 ERK1/2-induced myelin expansion results in increased conduction velocity (CV)

We hypothesized that the increased myelin thickness along with the changes in nodes of Ranvier would lead to increased conduction velocity (CV) in *Plp-Cre^{ERT};Mek1DD/+* mice. In particular, the observed shortening of the node length likely results in increased Na^+ channel clustering, leading to changes in axonal membrane ion permeability that affect the speed of signal propagation (Arancibia-Carcamo and Attwell, 2014). Since temporal accuracy is particularly critical in the auditory system (Seidl, 2014), we chose to measure *in vivo* auditory brainstem recordings (ABRs) to obtain a sensitive, non-invasive measure of potential electrophysiologic differences in 2 mpi *Plp-Cre^{ERT};Mek1DD/+* mice. Recording from five anatomical areas (I = auditory nerve, II = cochlear nucleus, III = cochlear nucleus/superior olivary complex, IV =

lateral lemniscus, V = inferior colliculus) along the auditory pathway uncovered a significant increase in CV in the CNS of *Plp-Cre^{ERT};Mek1DD/+* mice (Fig. 5A). Recordings made after 80 dB click stimulation showed significant decreases in absolute latency to peaks II (WT = 2.08 ± 0.06 ms, MUT = 1.90 ± 0.05 ms, p = 0.03), III (WT = 2.91 ± 0.03 ms, MUT = 2.79 ± 0.02 ms, p = 0.002), and V (WT = 4.84 ± 0.08 ms, MUT = 4.59 ± 0.08 ms, p = 0.04) of the CNS as visualized by a leftward shift for peaks II-V (corresponding to the CNS portions of the pathway) (Fig. 5A-B). Additionally, a significant decrease in the interpeak latency (IPL) between peaks I and V was observed (WT = 3.56 ± 0.06 ms, MUT = 3.34 ± 0.07 ms, p = 0.02) (Fig. 5C). These data provide evidence that ERK1/2-induced changes in myelin thickness have functional consequences, as they result in increased CV in the adult CNS.

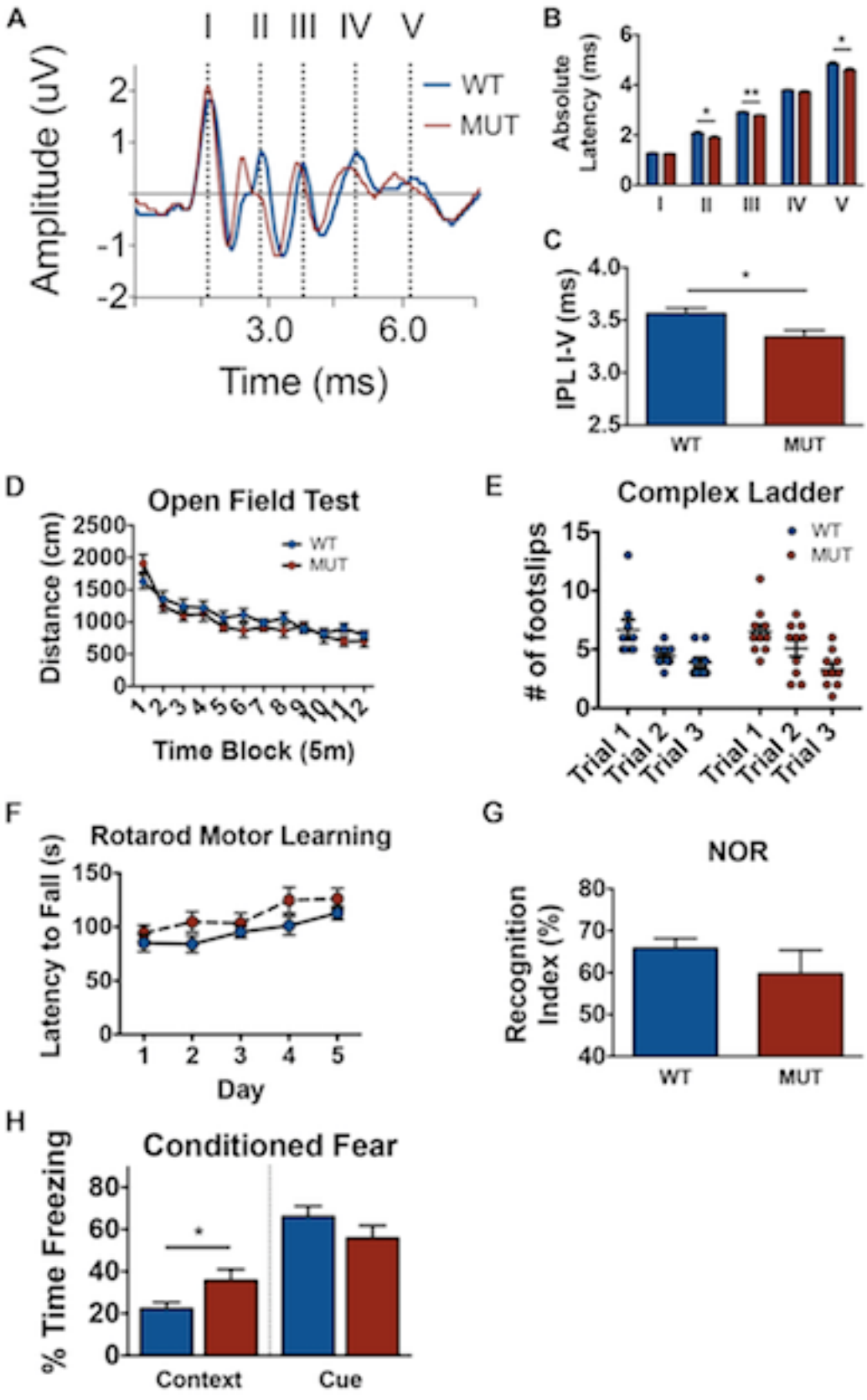
A
I II III IV V
Amplitude (uV)
2
1
-1
-2
3.0
6.0
Time (ms)
WT
MUT
B
Absolute Latency (ms)
6
4
2
0
I II III IV V
C
IPL I-V (ms)
4.0
3.5
3.0
2.5
WT
MUT
D
Open Field Test
Distance (cm)
2500
2000
1500
1000
500
0
WT
MUT
1 2 3 4 5 6 7 8 9 10 11 12
Time Block (5m)
E
Complex Ladder
# of footslips
15
10
5
0
WT
MUT
Trial 1
Trial 2
Trial 3
Trial 1
Trial 2
Trial 3
F
Rotarod Motor Learning
Latency to Fall (s)
150
100
50
0
1 2 3 4 5
Day
G
NOR
Recognition Index (%)
80
70
60
50
40
WT
MUT
H
Conditioned Fear
% Time Freezing
80
60
40
20
0
Context
Cue

Figure 5. ***Plp-Cre^{ERT};Mek1DD/+*** **mice exhibit increased conduction velocity in the CNS that does not significantly affect motor function but does enhance specific forms of hippocampal-based learning.**

A, Average auditory brainstem recording (ABR) traces from *WT;Mek1DD/+* (WT, blue) and *Plp-Cre^{ERT};Mek1DD/+* (MUT, red) mice at 2 mpi following 80dB click stimulation shows a visible leftward shift of the peaks in MUT mice, demonstrating increased conduction speed along axons. **B,** Quantification of results shown in **A** reveals a statistically significant decrease in the absolute latency to peaks II, III, and V of MUT (red) mice compared to WT (blue) controls. **C,** The interpeak latency following 16 kHz stimulation between peaks II-IV is also decreased in MUT (red) mice. **D,** Data from open field test shows no differences in the distance (cm) traveled over blocks of time (5 minutes each) between WT (blue) and MUT (red) mice at 2 mpi. **E,** Complex ladder analysis shows no significant differences in the number of footslips made by WT (blue) MUT (red) mice over 3 consecutive trials. **F,** Rotarod testing shows no differences between WT (blue) and MUT (red) mice in their latency to fall over the course of 5 training days, revealing no differences in motor coordination or learning. **G,** Novel object recognition (NOR) testing shows no difference in % time exploring the novel object between WT (blue) and MUT (red) mice, suggesting no differences in novelty discrimination. **H,** Conditioned fear data does not show a difference in % freezing between WT (blue) and MUT (red) mice in the cue trial, but does indicate a significant difference in % freezing between WT and MUT mice in the context trial. **$p<0.01$, *$p<0.05$. Data are mean ± SEM. Ten mice of each genotype were used for most analyses, including ABR trials; at least 7 mice of each genotype were used for behavioral analyses.

1.2.2 ERK1/2-induced hypermyelination leads to enhanced hippocampal-dependent emotional learning

Temporal accuracy of neuronal communication is essential to ensure appropriate information processing (Gerstner et al., 1997). The global hypermyelination and enhanced conduction velocity in the CNS seen in *Plp-Cre^{ERT};Mek1DD/+* mice might therefore improve learning and memory or motor skills. Alternatively, these changes might disrupt the delicate balance in signaling synchrony and lead to behavioral deficits. To address these possibilities, we performed behavioral tests focused on exploring both motor function and learning and memory. *Plp-Cre^{ERT};Mek1DD/+* mice showed general activity levels that were comparable to littermate controls when measured in an open field apparatus (Fig. 5D), and performed equally well compared to *WT;Mek1DD/+* controls when scored on the wire hang test (time hanging; WT = 44.7 ± 7.9 s, MUT = 40.0 ± 7.5 s, p = 0.67) and dowel walk test (side touches; WT = 6 ± 0.61, MUT = 6.5 ± 0.5, p = 0.45). These data suggest that ERK1/2-induced hypermyelination does not affect motor strength or coordination. Mutant mice also did not exhibit differences in number of footslips when scored on a complex ladder task over the course of three consecutive trials, showing similar motor coordination and working memory to control mice (Fig. 5E). Additionally, results from a motor learning accelerating rotarod assay did not reveal any significant differences between *WT;Mek1DD/+* and *Plp-Cre^{ERT};Mek1DD/+* mice in latency to fall on the initial day of testing (WT = 85.1 ± 8.1 s, MUT = 94.3 ± 7.2 s, p = 0.96) or over five days of training (Day 5, WT = 112.9 ± 6.2 s, MUT = 126.1 ± 9.8 s, p = 0.83), indicating that mutant mice do not have altered motor coordination or learning (Fig. 5F).

Plp-Cre^{ERT};Mek1DD/+ mice were next examined using novel object recognition (NOR), a classic memory test where mice tend to spend a greater percentage of time exploring a novel object over a familiar object. Mutant mice were found to perform comparably to *WT;Mek1DD/+* control littermates (Fig. 5G). To assess associative memory formation, we performed the conditioned fear (CF) test in *WT;Mek1DD/+* and *Plp-Cre^{ERT};Mek1DD/+* mice, in which a noxious stimulus (foot shock) is paired with a cue (tone) or with the surrounding context (environment). The successful association of these stimuli with the foot shock elicits a measurable fear freezing response from trained mice that are placed into the associated context or exposed to the associated cue 24 hours later. While mutant mice performed comparably to WT controls during the cue trial, a significant increase in freezing by *Plp-Cre^{ERT};Mek1DD/+* mice was observed after they were placed into a conditioned environment, suggesting that they experienced increased hippocampal-dependent associative emotional memory formation (Fig. 5H).

1.3 THE ROLE OF INCREASED ERK1/2 ACTIVATION IN MATURE OLIGODENDROCYTES IN REMYELINATION OF THE ADULT CNS

1.3.1 Preexisting OLs with sustained activation of ERK1/2 contribute to remyelination

Several studies have demonstrated that mature, pre-existing OLs do not normally contribute to myelin repair (Blakemore and Keirstead, 1999; Crawford et al., 2016; Keirstead and Blakemore, 1997). In order to determine whether forced activation of ERK1/2 in pre-existing mature OLs

enabled these cells to contribute to remyelination, we crossed *Plp-Cre^{ERT};Mek1DD/+* mice to a membrane bound GFP (mGFP) reporter strain (Hippenmeyer et al., 2005). Tamoxifen administered to ~3 month old *Plp-Cre^{ERT};+/+;mGFP* (control; CTRL) and *Plp-Cre^{ERT};Mek1DD/+;mGFP* (MUT) mice activated mGFP and *Mek1DD* expression in mutants and mGFP in control mice. Fourteen days later, demyelination was induced via lysolecithin (LPC) injection into the dorsal column of the thoracic spinal cord. This strategy enabled us to visualize and identify new myelin generated by pre-labeled surviving OLs following a demyelinating lesion. At 2 days post-lesion (dpl), both genotypes exhibited comparable lesions with very little mGFP or MBP immunoreactivity within the lesion, indicating a similar loss of pre-existing myelin (Fig. 6A,B). Small areas of mGFP and MBP immunoreactivity remained in mice of both genotypes likely due to incomplete clearance of myelin debris at this early time point. In support of previous work showing that enhanced activation of ERK1/2 in oligodendrocytes does not alter OL survival following LPC-induced demyelination (Fyffe-Maricich et al., 2013), we found similar numbers of oligodendrocyte lineage transcription factor 2 (OLIG2) positive cells in the lesioned dorsal column at 2 dpl (CTRL = 64.78 ± 14.09, MUT = 67 ± 13.09, p = 0.91) (Fig. 6C-D). To investigate whether there were changes in OPC proliferation in response to injury in the mutant mice, we administered the thymidine analog 5-ethylnyl-2'-deoxyuridine (EdU) to mice at 1 and 2 dpl before sacrifice, thereby labeling cycling cells across this time period via its incorporation into DNA during replication. We found that the percentage of EdU+ OLIG2+ cells in the lesioned dorsal column did not differ between *Plp-Cre^{ERT};+/+;mGFP* and *Plp-Cre^{ERT};Mek1DD/+;mGFP* mice (CTRL = 19.77 ± 0.84%, MUT = 25.04 ± 3.88%, p = 0.31) (Fig. 6C,E), indicating no significant differences in OPC proliferation similar to what has been previously reported in *CNP-Cre; Mek1DD* mice at 2dpl (Fyffe-Maricich et al., 2013). In

agreement with previous work showing that pre-existing OLs do not contribute to repair in wildtype mice (Crawford et al., 2016), *Plp-Cre^{ERT};+/+;mGFP* control mice exhibited very little mGFP+ myelin in the lesioned area at 42 dpl, when remyelination is virtually complete (Fig. 7A,B, left panels). In contrast, *Plp-Cre^{ERT};Mek1DD/+;mGFP* mice showed a dramatic increase in GFP+ immunoreactivity in the previously demyelinated area, particularly around the edges of the lesion (Fig. 7A,B, right panels). Small amounts of mGFP immunoreactivity were occasionally seen scattered throughout the lesion in control mice (Fig. 7D) because the *Plp* promoter is expressed in ~5% of OPCs in adult mice that are greater than 3 months old (Guo et al., 2010). Therefore, a very small fraction of myelin from newly generated OLs is green in both control and mutant mice. When mGFP+ regions in *Plp-Cre^{ERT};Mek1DD/+;mGFP* mice were examined at a higher magnification, colocalization of mGFP and MBP was apparent in rings around axons (Fig. 7D), suggesting that the sustained activation of ERK1/2 in pre-existing mature OLs enables them to contribute to remyelination. Areas of MBP+ but mGFP negative myelin rings in the *Plp-Cre^{ERT};Mek1DD/+;mGFP* mice (particularly near the center of the lesion), however, demonstrate that even though pre-existing OLs contributed to remyelination, a significant amount of myelin was still produced by newly generated OLs. Taken together, these data indicate that the sustained activation of ERK1/2 is sufficient to enable pre-existing OLs to extend processes into lesioned areas and contribute to myelin repair by wrapping axons.

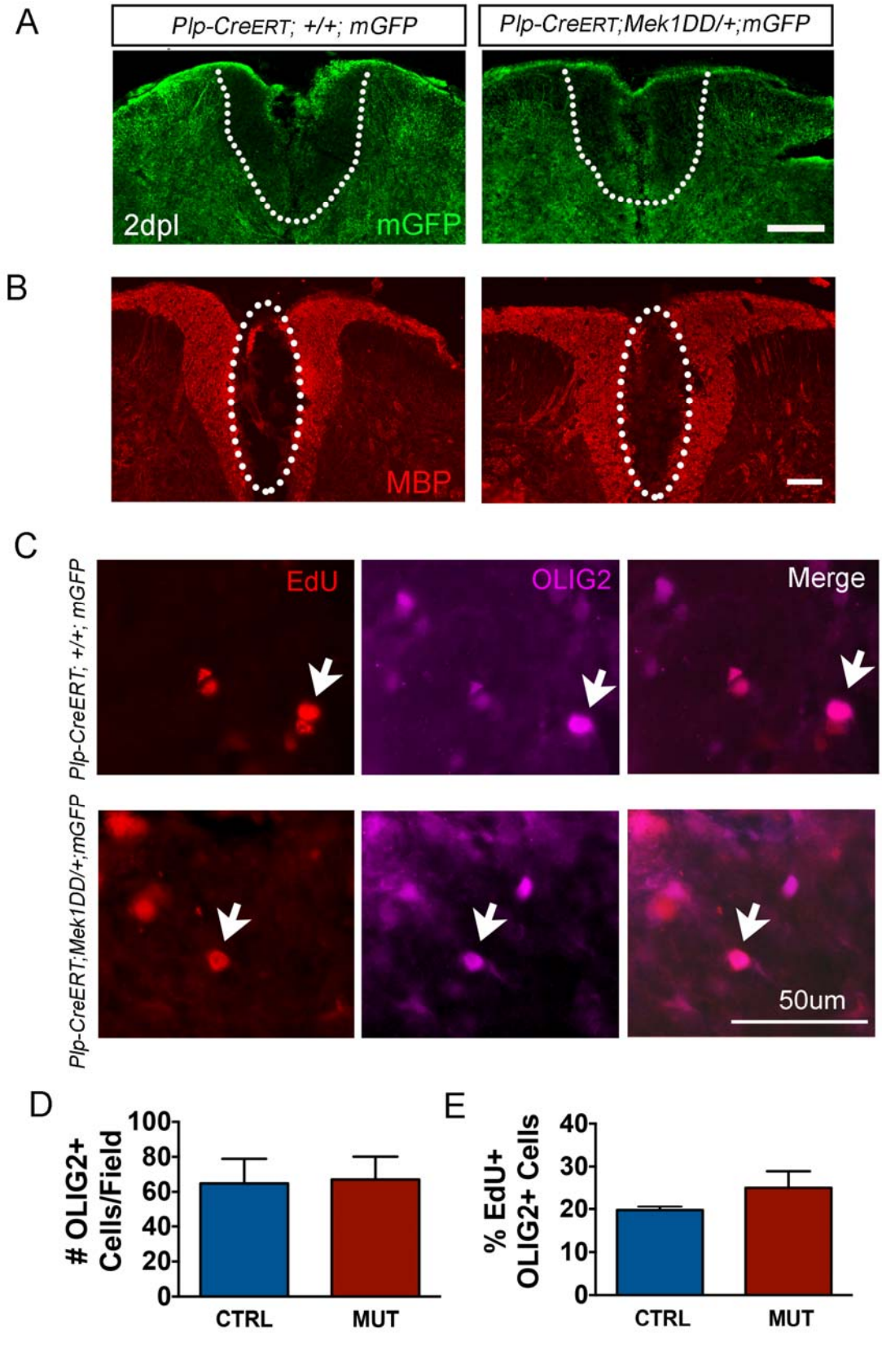
A
Plp-CreERT; +/+; mGFP
Plp-CreERT;Mek1DD/+;mGFP
2dpl
mGFP
B
MBP
C
EdU
OLIG2
Merge
Plp-CreERT; +/+; mGFP
Plp-CreERT;Mek1DD/+;mGFP
50um
D
OLIG2+ Cells/Field
100
80
60
40
20
0
CTRL
MUT
E
% EdU+ OLIG2+ Cells
40
30
20
10
0
CTRL
MUT

Figure 6. **Sustained activation of ERK1/2 in mature oligodendrocytes does not alter the immediate consequences of toxin-induced demyelination.**

A, Immunostaining with antibodies against mGFP at 2 days post- LPC lesion (2 dpl) indicates loss of pre-existing myelin (demyelination) leading to a lesioned area within the dorsal column of the spinal cord (SC). Scale bar, 100 µm. Dotted lines demarcate the dorsal column. **B,** MBP immunostaining at 2 dpl confirms an equivalent demyelinated area in the dorsal column of the SC in *Plp-Cre^{ERT};+/+, mGFP* and *Plp-Cre^{ERT};Mek1DD/+;mGFP* mice. Scale bar, 100 µm. Dotted elliptical demarcates the lesioned area. **C,** Co-labeling the lesioned dorsal column with EdU and OLIG2 reveals EdU+, OLIG2+ co-labeled cells. Scale bar, 50 µm. **D-E,** Sustained activation of ERK1/2 in OLs does not lead to a change in the total number of OLIG2+ cells or in the percentage of EdU+, OLIG2+ co-labeled cells divided by the total number of OLIG2+ cells at 2dpl, revealing no differences in OL survival or OPC proliferation between *Plp-Cre^{ERT};+/+, mGFP* (blue) and *Plp-Cre^{ERT};Mek1DD/+;mGFP* (red) mice. Three to five mice per genotype were used for all analyses.

Figure 7

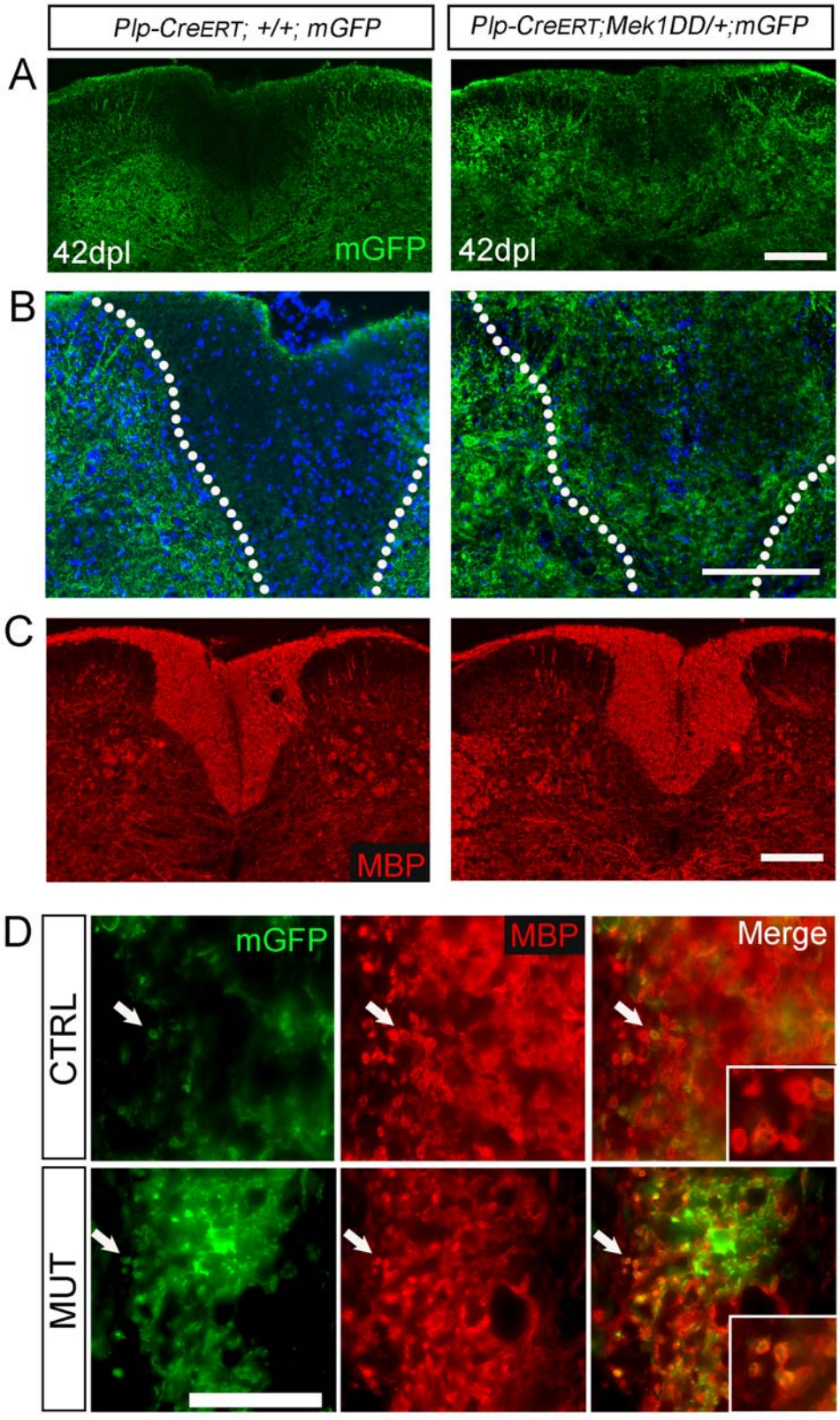
Plp-CreERT; +/+; mGFP
Plp-CreERT;Mek1DD/+;mGFP
A
42dpl
mGFP
42dpl
B
C
MBP
D
CTRL
MUT
mGFP
MBP
Merge

Figure 7. **Sustained activation of ERK1/2 in pre-existing mature oligodendrocytes enables them to contribute to remyelination following toxin-induced demyelination.**

A, At 42 dpl, control mice exhibit no visible mGFP+ process extension into the lesioned area, while *Plp-Cre^{ERT};Mek1DD/+;mGFP* mice show considerable mGFP+ process extension by pre-existing OLs into the previously demyelinated area. Scale bar, 100 µm. **B,** Higher magnification images of 42 dpl mGFP immunostaining further exemplifies data seen in **A**. DAPI marks cell nuclei in blue. Scale bar, 100 µm. Dorsal column is demarcated by dotted lines. **C,** MBP immunostaining at 42 dpl indicates complete remyelination in both *Plp-Cre^{ERT};+/+;mGFP* and *Plp-Cre^{ERT};Mek1DD/+;mGFP* spinal cord dorsal columns. Scale bar, 100 µm. **D,** MUT mice exhibit mGFP+ process extension into the lesioned area with nearby axons surrounded by MBP+, mGFP+ rings indicated by arrows (see also: inset panels); these appear rarely in WT controls. Scale bar, 50 µm. Three to five mice per genotype were used for all analyses.

1.4 DISCUSSION

1.4.1 Discussion

Synaptic plasticity and integration require that action potential arrival times occur with millisecond precision (Dan and Poo, 2006). Therefore, the regulation of conduction time is a critical variable for the formation and maintenance of important neuronal networks. Myelin greatly affects the speed of action potential propagation, promoting recent attention to how changes in myelin may contribute to nervous system plasticity, cognitive processing, and learning (recently reviewed by (Chang et al., 2016) and (Fields, 2015)). While it is widely

accepted that newly differentiated OLs contribute to myelin plasticity and repair, whether pre-existing OLs can also lead to functional changes in both the injured and uninjured adult CNS remains unknown. In this study we used transgenic mice with sustained activation of ERK1/2 in mature OLs to demonstrate that pre-existing OLs can re-initiate active myelination in the adult CNS, resulting in increased conduction velocity that leads to enhanced contextual fear learning and contributes to remyelination.

Increased levels of pERK1/2 trigger myelin growth that results in global CNS hypermyelination. We determined that this hypermyelination was mediated primarily by pre-existing OLs since increasing pERK1/2 in adult OPCs, but not pre-existing OLs, did not lead to white matter expansion. Interestingly, the majority of myelin growth occurs within the first 21 days after ERK1/2 activation and the accompanying white matter expansion is more robust in the spinal cord compared to the corpus callosum. Myelin thickness continues to increase over time but does so at such a slow rate that even after 2-3 months, the modest accumulation of myelin does not appear to become pathologic. These data are in contrast to the excessive myelin overgrowth and abnormalities observed in transgenic mice that overexpress AKT (Flores et al., 2008), lack PTEN (Harrington et al., 2010), or over-activate MAPK signaling in the peripheral nervous system (Sheean et al., 2014). It is possible that inhibitory factors such as phosphatases provide continuous negative regulation of ERK1/2 signaling by counteracting the effects of constitutively active MEK1; further studies are needed to address this issue.

Re-initiation of myelination seen in adult *Plp-Cre^{ERT};Mek1DD/+* mice supports the earlier finding that myelin growth can be experimentally reactivated in adult mice by conditionally deleting PTEN to activate PI3K/AKT signaling (Goebbels et al., 2010). How is it that new myelin membrane can be added to previously formed sheaths? Recent studies show that

an elaborate system of cytoplasmic channels exists within the growing myelin sheath to enable the trafficking of newly synthesized myelin membrane components to the leading edge of the expanding sheath (Snaidero et al., 2014). Importantly, these channels are dynamic and can reopen during adulthood in response to PI3K activation along with elevated levels of its lipid product phosphatidyl inositol triphosphate (PI(3,4,5)P3) (Snaidero et al., 2014). Additionally, new myelin growth appears to be driven from the inner tongue as a result of actin cytoskeleton rearrangement (Snaidero et al., 2014; Zuchero et al., 2015) and it has been hypothesized that release of gelsolin and cofilin from membrane-bound PIP2 triggers actin depolymerization necessary for myelin wrapping (Zuchero et al., 2015). It is possible that ERK1/2 signaling similarly drives myelin wrapping through the regulation of actin dynamics. Furthermore, the parallel consequences of upregulating or downregulating PI3K/AKT/mTOR and ERK1/2 signaling pathways on myelination during development (Bercury et al., 2014; Flores et al., 2008; Goebbels et al., 2010; Ishii et al., 2013; Ishii et al., 2012; Lebrun-Julien et al., 2014; Wahl et al., 2014) suggests significant crosstalk between these two pathways (Dai et al., 2014; Gaesser and Fyffe-Maricich, 2016). While the mechanisms behind how ERK1/2 drives myelin wrapping remain unclear, it seems likely that this pathway acts in conjunction with PI3K/AKT/mTOR signaling at multiple points of convergence to regulate myelination. The specific mechanisms and downstream targets of ERK1/2 that control myelin wrapping represent important areas for future research.

New findings suggest that myelin abnormalities occur in a variety of psychiatric illnesses and neurodevelopmental disorders, such as autism, implicating myelin in cognitive function (Fields, 2008; Liu et al., 2012; Makinodan et al., 2012). The correlation of myelin abnormalities with cognitive deficits in these diseases, however, is complicated by the fact that significant

primary neuronal dysfunction occurs concurrently. Here, our genetic mouse model of ERK1/2-mediated hypermyelination provided a unique opportunity to assess the consequences of primary increases in myelin thickness on mouse behavior in the absence of significant neuronal pathology. Cognitive function testing using the novel object recognition assay (NOR) revealed that mutants performed comparably to control littermates. NOR is an established test of recognition memory involving the hippocampus and portions of the medial temporal lobe, such as the perirhinal cortex and parahippocampal gyrus (Antunes and Biala, 2012). Short-term retention intervals similar to what we used in this study are thought to primarily involve hippocampal-independent mechanisms of recognition (Balderas et al., 2008; Hammond et al., 2004; Oliveira et al., 2010). Therefore our data suggest that hippocampal-independent recognition memory is unaffected by ERK1/2-induced hypermyelination. Conditioned fear testing focuses on long-term learning and memory based in the hippocampus and amygdala and relies on the association of a cue or environment with a noxious stimulus (foot shock) (Phillips and LeDoux, 1992). Interestingly, the conditioned freezing response is known to depend on activity-dependent plasticity mechanisms (Fanselow and Kim, 1994; Maren et al., 2003; Rozeske et al., 2015; Sindreu et al., 2007). *Plp-Cre^{ERT};Mek1DD/+* mice did not exhibit changes in freezing during the cue trial, indicating no abnormalities in memory formation involving the amygdala. In the context trial which relies heavily on hippocampal-based memory formation (Sanders et al., 2003), however, mutant mice exhibited significantly increased freezing, suggesting that hippocampal-based emotional memory is enhanced in mice with ERK1/2-induced hypermyelination. Future studies will address why the hippocampus seems to be more sensitive to increased myelination compared to other structures. Additional experiments

investigating the consequences of hypermyelination on more complex behaviors such as social interaction, anxiety, and depression are currently underway.

Surprisingly, *Plp-Cre^{ERT};Mek1DD/+* mice did not exhibit changes in general activity or motor coordination and strength, despite a significant expansion of the spinal cord white matter. Together, the results from our behavioral analyses demonstrate that subtle global hypermyelination does not lead to obvious motor or cognitive deficits. Despite increased myelin thickness and accompanied faster conduction speeds, it seems that the synchronicity of impulses was not sufficiently altered to negatively affect a number of behaviors in the *Plp-Cre^{ERT};Mek1DD/+* mice. These data are in contrast to the detrimental effects that occur following the loss of myelin, including deficits in motor function, social behavior, and cognitive function (Fields, 2008; Gootjes et al., 2004; Ishii et al., 2014; Kujala et al., 1997; Liu et al., 2012; Makinodan et al., 2012). The fact that the CNS appears to be somewhat tolerant of global increases in myelin thickness is promising from a therapeutic standpoint. For example, in patients with multiple sclerosis, demyelinated lesions appear throughout the CNS and are variable in their location. Without invasive brain surgery, even specialized small molecule therapeutics targeting the OL population would inevitably lead to new myelin production in both affected and unaffected areas throughout the CNS.

In addition to positive effects on associative emotional memory formation, the ability to re-initiate myelination appears beneficial in the context of demyelinating injury. We show that pre-existing OLs do not normally contribute to remyelination, a finding that agrees with data from a number of previous studies (Blakemore and Keirstead, 1999; Carroll et al., 1998; Crawford et al., 2016; Gensert and Goldman, 1997; Keirstead and Blakemore, 1997), but that sustained ERK1/2 activation enables them to extend process into the lesion area and contribute to

remyelination. Studies are currently underway to determine whether these MBP+, mGFP+ wraps contribute in a functional way to the process of myelin repair. Although surviving OLs in *Plp-Cre^{ERT};Mek1DD/+;mGFP* mice were clearly able to extend processes that surround axons within the area of demyelination, a large number of remyelinated axons were covered by MBP positive, mGFP negative wraps (particularly in the center of the lesioned area where pre-existing OLs do not survive), demonstrating that they were generated by newly generated OLs. This suggests that myelin generated solely by pre-existing OLs is unlikely to be sufficient for complete remyelination, and that any strategy designed to harness the potential of these pre-existing cells should also aim to target newly generated OLs. Fortunately, *CNP-Cre;Mek1DD* mice that have increased levels of pERK1/2 in both pre-existing and newly generated OLs show accelerated myelin repair after injury and are able to generate thick myelin sheaths around remyelinated axons (Fyffe-Maricich et al., 2013). In light of our observations here, it is tempting to speculate that myelin generated by both pre-existing and newly born OLs contributed to the enhanced myelin repair seen in *CNP-Cre;Mek1DD* mice.

In summary, our results illuminate the potential of downstream effectors in the ERK1/2 signaling pathway as novel therapeutic targets for enhancing myelin plasticity and myelin repair in a broad range of neural disorders. Future work will focus on determining these key OL-specific ERK1/2 downstream targets.

BIBLIOGRAPHY

Antunes, M., and Biala, G. (2012). The novel object recognition memory: neurobiology, test procedure, and its modifications. Cogn Process *13*, 93-110.

Arancibia-Carcamo, I.L., and Attwell, D. (2014). The node of Ranvier in CNS pathology. Acta Neuropathol *128*, 161-175.

Balderas, I., Rodriguez-Ortiz, C.J., Salgado-Tonda, P., Chavez-Hurtado, J., McGaugh, J.L., and Bermudez-Rattoni, F. (2008). The consolidation of object and context recognition memory involve different regions of the temporal lobe. Learn Mem *15*, 618-624.

Bartsch, S., Montag, D., Schachner, M., and Bartsch, U. (1997). Increased number of unmyelinated axons in optic nerves of adult mice deficient in the myelin-associated glycoprotein (MAG). Brain Res *762*, 231-234.

Bengtsson, S.L., Nagy, Z., Skare, S., Forsman, L., Forssberg, H., and Ullen, F. (2005). Extensive piano practicing has regionally specific effects on white matter development. Nat Neurosci *8*, 1148-1150.

Bercury, K.K., Dai, J., Sachs, H.H., Ahrendsen, J.T., Wood, T.L., and Macklin, W.B. (2014). Conditional ablation of raptor or rictor has differential impact on oligodendrocyte differentiation and CNS myelination. J Neurosci *34*, 4466-4480.

Blakemore, W.F., and Keirstead, H.S. (1999). The origin of remyelinating cells in the central nervous system. J Neuroimmunol *98*, 69-76.

Carroll, W.M., Jennings, A.R., and Ironside, L.J. (1998). Identification of the adult resting progenitor cell by autoradiographic tracking of oligodendrocyte precursors in experimental CNS demyelination. Brain *121 (Pt 2)*, 293-302.

Chang, A., Tourtellotte, W.W., Rudick, R., and Trapp, B.D. (2002). Premyelinating oligodendrocytes in chronic lesions of multiple sclerosis. N Engl J Med *346*, 165-173.

Chang, K.J., Redmond, S.A., and Chan, J.R. (2016). Remodeling myelination: implications for mechanisms of neural plasticity. Nat Neurosci *19*, 190-197.

Crawford, A.H., Tripathi, R.B., Foerster, S., McKenzie, I., Kougioumtzidou, E., Grist, M., Richardson, W.D., and Franklin, R.J. (2016). Pre-Existing Mature Oligodendrocytes Do Not Contribute to Remyelination following Toxin-Induced Spinal Cord Demyelination. Am J Pathol *186*, 511-516.

Dai, J., Bercury, K.K., and Macklin, W.B. (2014). Interaction of mTOR and Erk1/2 signaling to regulate oligodendrocyte differentiation. Glia *62*, 2096-2109.

Dan, Y., and Poo, M.M. (2006). Spike timing-dependent plasticity: from synapse to perception. Physiol Rev *86*, 1033-1048.

Dangata, Y.Y., and Kaufman, M.H. (1997). Myelinogenesis in the optic nerve of (C57BL x CBA) F1 hybrid mice: a morphometric analysis. Eur J Morphol *35*, 3-17.

Dawson, M.R., Polito, A., Levine, J.M., and Reynolds, R. (2003). NG2-expressing glial progenitor cells: an abundant and widespread population of cycling cells in the adult rat CNS. Mol Cell Neurosci *24*, 476-488.

Demerens, C., Stankoff, B., Logak, M., Anglade, P., Allinquant, B., Couraud, F., Zalc, B., and Lubetzki, C. (1996). Induction of myelination in the central nervous system by electrical activity. Proc Natl Acad Sci U S A *93*, 9887-9892.

Dimou, L., Simon, C., Kirchhoff, F., Takebayashi, H., and Gotz, M. (2008). Progeny of Olig2-expressing progenitors in the gray and white matter of the adult mouse cerebral cortex. J Neurosci *28*, 10434-10442.

Doerflinger, N.H., Macklin, W.B., and Popko, B. (2003). Inducible site-specific recombination in myelinating cells. Genesis *35*, 63-72.

Fancy, S.P., Zhao, C., and Franklin, R.J. (2004). Increased expression of Nkx2.2 and Olig2 identifies reactive oligodendrocyte progenitor cells responding to demyelination in the adult CNS. Mol Cell Neurosci *27*, 247-254.

Fanselow, M.S., and Kim, J.J. (1994). Acquisition of contextual Pavlovian fear conditioning is blocked by application of an NMDA receptor antagonist D,L-2-amino-5-phosphonovaleric acid to the basolateral amygdala. Behav Neurosci *108*, 210-212.

Farr, T.D., Liu, L., Colwell, K.L., Whishaw, I.Q., and Metz, G.A. (2006). Bilateral alteration in stepping pattern after unilateral motor cortex injury: a new test strategy for analysis of skilled limb movements in neurological mouse models. J Neurosci Methods *153*, 104-113.

Fields, R.D. (2008). White matter in learning, cognition and psychiatric disorders. Trends Neurosci *31*, 361-370.

Fields, R.D. (2015). A new mechanism of nervous system plasticity: activity-dependent myelination. Nat Rev Neurosci *16*, 756-767.

Flores, A.I., Narayanan, S.P., Morse, E.N., Shick, H.E., Yin, X., Kidd, G., Avila, R.L., Kirschner, D.A., and Macklin, W.B. (2008). Constitutively active Akt induces enhanced myelination in the CNS. J Neurosci *28*, 7174-7183.

Fyffe-Maricich, S.L., Schott, A., Karl, M., Krasno, J., and Miller, R.H. (2013). Signaling through ERK1/2 controls myelin thickness during myelin repair in the adult central nervous system. J Neurosci *33*, 18402-18408.

Gaesser, J.M., and Fyffe-Maricich, S.L. (2016). Intracellular signaling pathway regulation of myelination and remyelination in the CNS. Exp Neurol.

Gensert, J.M., and Goldman, J.E. (1997). Endogenous progenitors remyelinate demyelinated axons in the adult CNS. Neuron *19*, 197-203.

Gerstner, W., Kreiter, A.K., Markram, H., and Herz, A.V. (1997). Neural codes: firing rates and beyond. Proc Natl Acad Sci U S A *94*, 12740-12741.

Goebbels, S., Oltrogge, J.H., Kemper, R., Heilmann, I., Bormuth, I., Wolfer, S., Wichert, S.P., Mobius, W., Liu, X., Lappe-Siefke, C.*, et al.* (2010). Elevated phosphatidylinositol 3,4,5-trisphosphate in glia triggers cell-autonomous membrane wrapping and myelination. J Neurosci *30*, 8953-8964.

Gootjes, L., Teipel, S.J., Zebuhr, Y., Schwarz, R., Leinsinger, G., Scheltens, P., Moller, H.J., and Hampel, H. (2004). Regional distribution of white matter hyperintensities in vascular dementia, Alzheimer's disease and healthy aging. Dement Geriatr Cogn Disord *18*, 180-188.

Guo, F., Maeda, Y., Ma, J., Xu, J., Horiuchi, M., Miers, L., Vaccarino, F., and Pleasure, D. (2010). Pyramidal neurons are generated from oligodendroglial progenitor cells in adult piriform cortex. J Neurosci *30*, 12036-12049.

Hammond, R.S., Tull, L.E., and Stackman, R.W. (2004). On the delay-dependent involvement of the hippocampus in object recognition memory. Neurobiol Learn Mem *82*, 26-34.

Harrington, E.P., Zhao, C., Fancy, S.P., Kaing, S., Franklin, R.J., and Rowitch, D.H. (2010). Oligodendrocyte PTEN is required for myelin and axonal integrity, not remyelination. Ann Neurol *68*, 703-716.

Hippenmeyer, S., Vrieseling, E., Sigrist, M., Portmann, T., Laengle, C., Ladle, D.R., and Arber, S. (2005). A developmental switch in the response of DRG neurons to ETS transcription factor signaling. PLoS Biol *3*, e159.

Honjin, R., Sakato, S., and Yamashita, T. (1977). Electron microscopy of the mouse optic nerve: a quantitative study of the total optic nerve fibers. Arch Histol Jpn *40*, 321-332.

Ishii, A., Furusho, M., and Bansal, R. (2013). Sustained activation of ERK1/2 MAPK in oligodendrocytes and schwann cells enhances myelin growth and stimulates oligodendrocyte progenitor expansion. J Neurosci *33*, 175-186.

Ishii, A., Furusho, M., Dupree, J.L., and Bansal, R. (2014). Role of ERK1/2 MAPK signaling in the maintenance of myelin and axonal integrity in the adult CNS. J Neurosci *34*, 16031-16045.

Ishii, A., Fyffe-Maricich, S.L., Furusho, M., Miller, R.H., and Bansal, R. (2012). ERK1/ERK2 MAPK signaling is required to increase myelin thickness independent of oligodendrocyte differentiation and initiation of myelination. J Neurosci *32*, 8855-8864.

Kang, S.H., Fukaya, M., Yang, J.K., Rothstein, J.D., and Bergles, D.E. (2010). NG2+ CNS glial progenitors remain committed to the oligodendrocyte lineage in postnatal life and following neurodegeneration. Neuron *68*, 668-681.

Keirstead, H.S., and Blakemore, W.F. (1997). Identification of post-mitotic oligodendrocytes incapable of remyelination within the demyelinated adult spinal cord. J Neuropathol Exp Neurol *56*, 1191-1201.

Kujala, P., Portin, R., and Ruutiainen, J. (1997). The progress of cognitive decline in multiple sclerosis. A controlled 3-year follow-up. Brain *120 (Pt 2)*, 289-297.

Lebrun-Julien, F., Bachmann, L., Norrmen, C., Trotzmuller, M., Kofeler, H., Ruegg, M.A., Hall, M.N., and Suter, U. (2014). Balanced mTORC1 activity in oligodendrocytes is required for accurate CNS myelination. J Neurosci *34*, 8432-8448.

Liu, J., Dietz, K., DeLoyht, J.M., Pedre, X., Kelkar, D., Kaur, J., Vialou, V., Lobo, M.K., Dietz, D.M., Nestler, E.J., *et al.* (2012). Impaired adult myelination in the prefrontal cortex of socially isolated mice. Nat Neurosci *15*, 1621-1623.

Makinodan, M., Rosen, K.M., Ito, S., and Corfas, G. (2012). A critical period for social experience-dependent oligodendrocyte maturation and myelination. Science *337,* 1357-1360.

Maren, S., Ferrario, C.R., Corcoran, K.A., Desmond, T.J., and Frey, K.A. (2003). Protein synthesis in the amygdala, but not the auditory thalamus, is required for consolidation of Pavlovian fear conditioning in rats. Eur J Neurosci *18*, 3080-3088.

McKenzie, I.A., Ohayon, D., Li, H., de Faria, J.P., Emery, B., Tohyama, K., and Richardson, W.D. (2014). Motor skill learning requires active central myelination. Science *346*, 318-322.

Michel, K., Zhao, T., Karl, M., Lewis, K., and Fyffe-Maricich, S.L. (2015). Translational control of myelin basic protein expression by ERK2 MAP kinase regulates timely remyelination in the adult brain. J Neurosci *35*, 7850-7865.

Norton, W.T., and Cammer, W. (1984). Isolation and Characterization of Myelin. In Myelin, P. Morell, ed. (Springer US), pp. 147-195.

Oliveira, A.M., Hawk, J.D., Abel, T., and Havekes, R. (2010). Post-training reversible inactivation of the hippocampus enhances novel object recognition memory. Learn Mem *17*, 155-160.

Phillips, R.G., and LeDoux, J.E. (1992). Differential contribution of amygdala and hippocampus to cued and contextual fear conditioning. Behav Neurosci *106*, 274-285.

Psachoulia, K., Jamen, F., Young, K.M., and Richardson, W.D. (2009). Cell cycle dynamics of NG2 cells in the postnatal and ageing brain. Neuron Glia Biol *5*, 57-67.

Rivers, L.E., Young, K.M., Rizzi, M., Jamen, F., Psachoulia, K., Wade, A., Kessaris, N., and Richardson, W.D. (2008). PDGFRA/NG2 glia generate myelinating oligodendrocytes and piriform projection neurons in adult mice. Nat Neurosci *11*, 1392-1401.

Rozeske, R.R., Valerio, S., Chaudun, F., and Herry, C. (2015). Prefrontal neuronal circuits of contextual fear conditioning. Genes Brain Behav *14*, 22-36.

Sanders, M.J., Wiltgen, B.J., and Fanselow, M.S. (2003). The place of the hippocampus in fear conditioning. Eur J Pharmacol *463*, 217-223.

Schlegel, A.A., Rudelson, J.J., and Tse, P.U. (2012). White matter structure changes as adults learn a second language. J Cogn Neurosci *24*, 1664-1670.

Scholz, J., Klein, M.C., Behrens, T.E., and Johansen-Berg, H. (2009). Training induces changes in white-matter architecture. Nat Neurosci *12*, 1370-1371.

Seidl, A.H. (2014). Regulation of conduction time along axons. Neuroscience *276*, 126-134.

Sheean, M.E., McShane, E., Cheret, C., Walcher, J., Muller, T., Wulf-Goldenberg, A., Hoelper, S., Garratt, A.N., Kruger, M., Rajewsky, K.*, et al.* (2014). Activation of MAPK overrides the termination of myelin growth and replaces Nrg1/ErbB3 signals during Schwann cell development and myelination. Genes Dev *28*, 290-303.

Sim, F.J., Zhao, C., Penderis, J., and Franklin, R.J. (2002). The age-related decrease in CNS remyelination efficiency is attributable to an impairment of both oligodendrocyte progenitor recruitment and differentiation. The Journal of neuroscience : the official journal of the Society for Neuroscience *22*, 2451-2459.

Sindreu, C.B., Scheiner, Z.S., and Storm, D.R. (2007). Ca2+ -stimulated adenylyl cyclases regulate ERK-dependent activation of MSK1 during fear conditioning. Neuron *53*, 79-89.

Snaidero, N., Mobius, W., Czopka, T., Hekking, L.H., Mathisen, C., Verkleij, D., Goebbels, S., Edgar, J., Merkler, D., Lyons, D.A.*, et al.* (2014). Myelin membrane wrapping of CNS axons by PI(3,4,5)P3-dependent polarized growth at the inner tongue. Cell *156*, 277-290.

Srinivasan, L., Sasaki, Y., Calado, D.P., Zhang, B., Paik, J.H., DePinho, R.A., Kutok, J.L., Kearney, J.F., Otipoby, K.L., and Rajewsky, K. (2009). PI3 kinase signals BCR-dependent mature B cell survival. Cell *139*, 573-586.

Stevens, B., Porta, S., Haak, L.L., Gallo, V., and Fields, R.D. (2002). Adenosine: a neuron-glial transmitter promoting myelination in the CNS in response to action potentials. Neuron *36,* 855-868.

Stevens, B., Tanner, S., and Fields, R.D. (1998). Control of myelination by specific patterns of neural impulses. J Neurosci *18*, 9303-9311.

Sturrock, R.R. (1980). Myelination of the mouse corpus callosum. Neuropathol Appl Neurobiol *6*, 415-420.

Tripathi, R.B., Rivers, L.E., Young, K.M., Jamen, F., and Richardson, W.D. (2010). NG2 glia generate new oligodendrocytes but few astrocytes in a murine experimental autoimmune encephalomyelitis model of demyelinating disease. J Neurosci *30*, 16383-16390.

Wahl, S.E., McLane, L.E., Bercury, K.K., Macklin, W.B., and Wood, T.L. (2014). Mammalian target of rapamycin promotes oligodendrocyte differentiation, initiation and extent of CNS myelination. J Neurosci *34*, 4453-4465.

Wake, H., Lee, P.R., and Fields, R.D. (2011). Control of local protein synthesis and initial events in myelination by action potentials. Science *333*, 1647-1651.

Wang, H., Yin, G., Rogers, K., Miralles, C., De Blas, A.L., and Rubio, M.E. (2011). Monaural conductive hearing loss alters the expression of the GluA3 AMPA and glycine receptor alpha1 subunits in bushy and fusiform cells of the cochlear nucleus. Neuroscience *199*, 438-451.

Waxman, S.G. (1980). Determinants of conduction velocity in myelinated nerve fibers. Muscle Nerve *3*, 141-150.

Waxman, S.G. (1997). Axon-glia interactions: building a smart nerve fiber. Curr Biol *7*, R406-410.

Yeung, M.S., Zdunek, S., Bergmann, O., Bernard, S., Salehpour, M., Alkass, K., Perl, S., Tisdale, J., Possnert, G., Brundin, L.*, et al.* (2014). Dynamics of oligodendrocyte generation and myelination in the human brain. Cell *159*, 766-774.

Young, K.M., Psachoulia, K., Tripathi, R.B., Dunn, S.J., Cossell, L., Attwell, D., Tohyama, K., and Richardson, W.D. (2013). Oligodendrocyte dynamics in the healthy adult CNS: evidence for myelin remodeling. Neuron *77*, 873-885.

Zawadzka, M., Rivers, L.E., Fancy, S.P., Zhao, C., Tripathi, R., Jamen, F., Young, K., Goncharevich, A., Pohl, H., Rizzi, M.*, et al.* (2010). CNS-resident glial progenitor/stem cells

produce Schwann cells as well as oligodendrocytes during repair of CNS demyelination. Cell Stem Cell *6*, 578-590.

Zuchero, J.B., Fu, M.M., Sloan, S.A., Ibrahim, A., Olson, A., Zaremba, A., Dugas, J.C., Wienbar, S., Caprariello, A.V., Kantor, C.*, et al.* (2015). CNS myelin wrapping is driven by actin disassembly. Dev Cell *34*, 152-167.